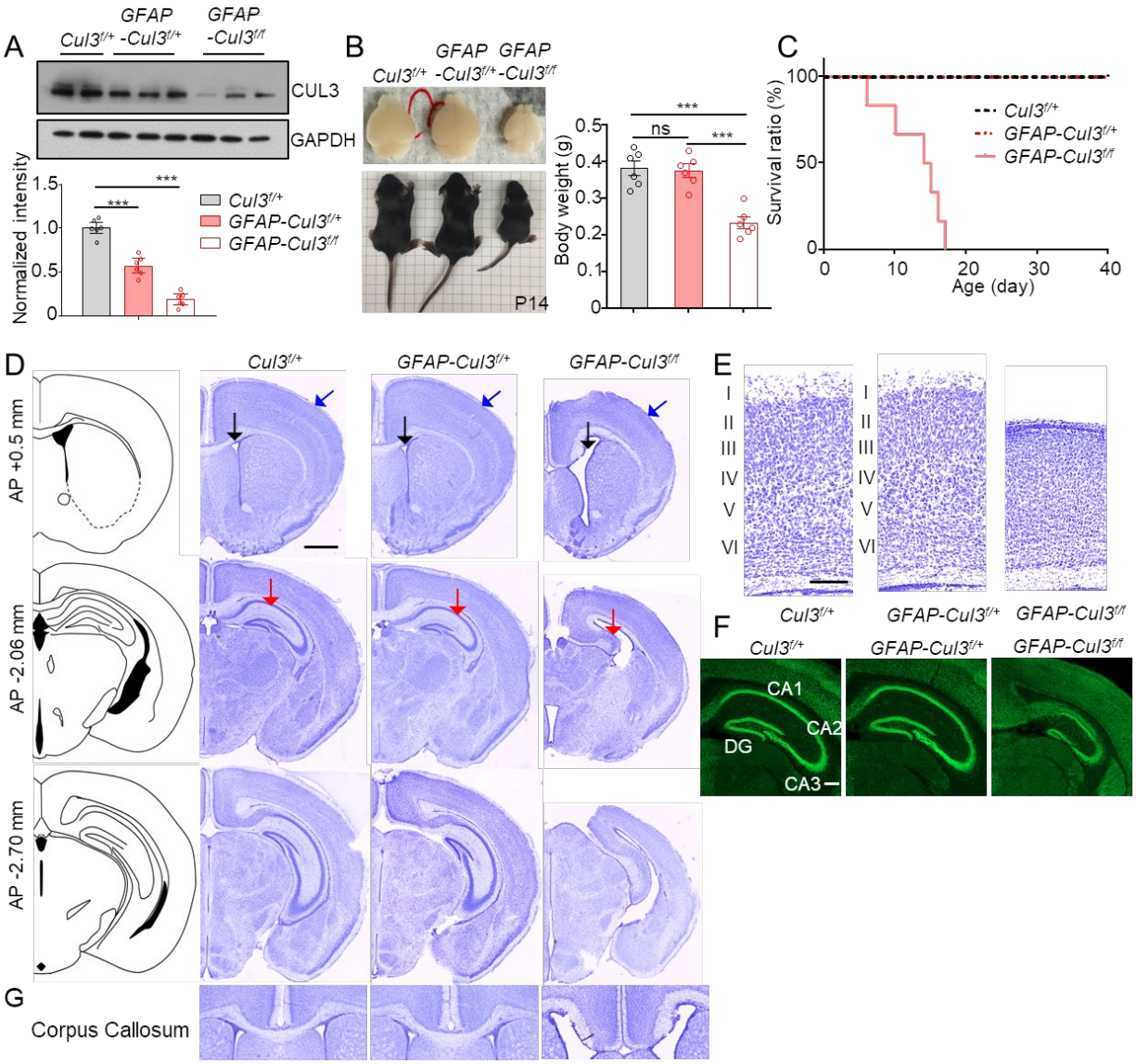

Figure S1. Premature death and brain deficits in *GFAP-Cul3$^{f/f}$* mice. Related to Figure 1. (A) Reduced CUL3 level in *GFAP-Cul3$^{f/+}$* and *GFAP-Cul3$^{f/f}$* mice. Brains were isolated from P14 mice and blotted for CUL3. n = 6 mice for each genotype; *Cul3$^{f/+}$* (1.0 ± 0.07) vs *GFAP-Cul3$^{f/+}$* (0.5 ± 0.11), $p < 0.0001$; *Cul3$^{f/+}$* vs *GFAP-Cul3$^{f/f}$* (0.2 ± 0.08), $p < 0.0001$; $F_{(2,15)} = 127.6$, $p < 0.0001$; One-way ANOVA followed by Tukey's post hoc test. (B) Reduced brain size and body weight in *GFAP-Cul3$^{f/f}$* mice at the age of P14 (n = 6 mice for each genotype; *Cul3$^{f/+}$* (0.4 ± 0.02 g) vs *GFAP-Cul3$^{f/f}$* (0.2 ± 0.02 g), $p < 0.0001$; *GFAP-Cul3$^{f/+}$* (0.4 ± 0.02 g) vs *GFAP-Cul3$^{f/f}$*, $p = 0.0001$; $F_{(2,15)} = 22.75$, $p < 0.0001$; One-way ANOVA followed by Tukey's post hoc test. (C) Reduced lifespan of *GFAP-Cul3$^{f/f}$* mice. (D-G) Enlarged ventricles, Scale bar, 1 mm (D), reduced cortical thickness, Scale bar, 100 μm (E), deformed hippocampus Scale bar, 500 μm (F) and agenesis of the corpus callosum (G). Data were shown as mean ± SEM. *$p < 0.05$, **$p < 0.01$, ***$p < 0.001$; ns, no significant difference.

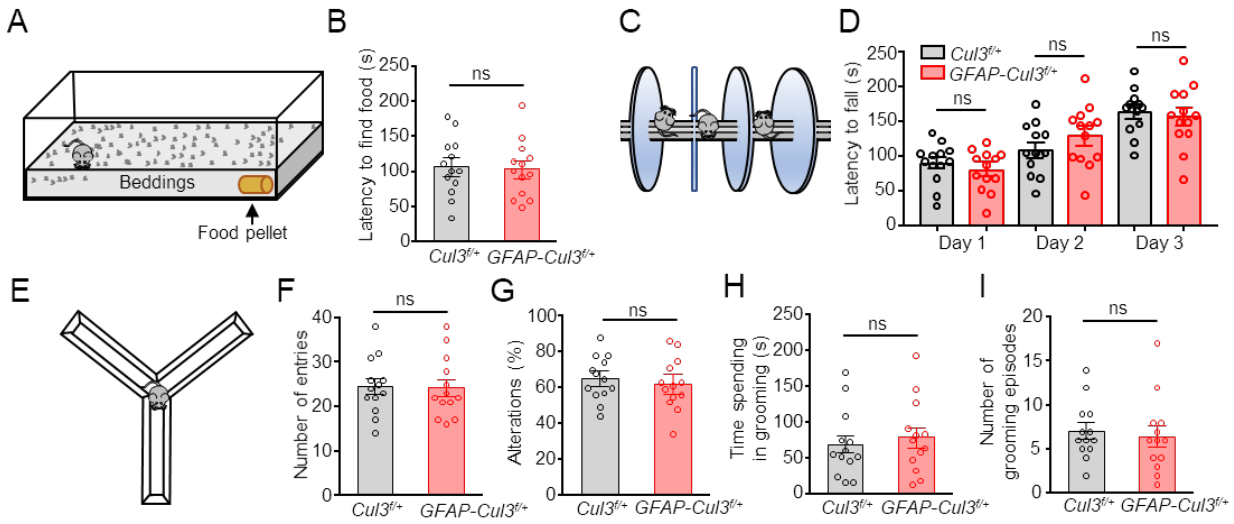

Figure S2. *GFAP-Cul3$^{f/+}$* mice did not show difference in motor function, grooming, working memory and olfactory behavior. Related to Figure 1. (A) Schematic diagram for buried food-seeking tests. (B) Normal food finding in buried food-seeking tests. n = 13 mice for each genotype; p = 0.7911; *U* = 79; Mann-Whitney test. (C) Schematic diagram for accelerated rotarod tests. (D) Normal motor performance in accelerated rotarod test. n = 13 mice for each genotype; *Cul3$^{f/+}$* vs *GFAP-Cul3$^{f/+}$* on Day 1, p = 0.4401, U= 69; *Cul3$^{f/+}$* vs *GFAP-Cul3$^{f/+}$* on Day 2, p = 0.2807, U = 63; *Cul3$^{f/+}$* vs *GFAP-Cul3$^{f/+}$* on Day 3, p = 0.5193, U = 71.5; Mann-Whitney test. (E) Schematic diagram for Y-maze tests. (F) Unaltered arms entries in Y-maze tests. n = 13 mice for each genotype; p = 0.6761; *U* = 76; Mann-Whitney test. (G) Unaltered alterations percentile in Y-maze tests. n = 13 mice for each genotype; p = 0.5528; *U* = 72.5; Mann-Whitney test. (H) Unaltered grooming time during 15 min home cage activity. n = 13 mice for each genotype; p = 0.4871; *U* = 70.5; Mann-Whitney test. (I) Unaltered number of grooming episodes during 15 min home cage activity. n = 13 mice for each genotype; p = 0.5167; *U* = 71.5; Mann-Whitney test. Data were shown as mean ± SEM. ns, no significant difference.

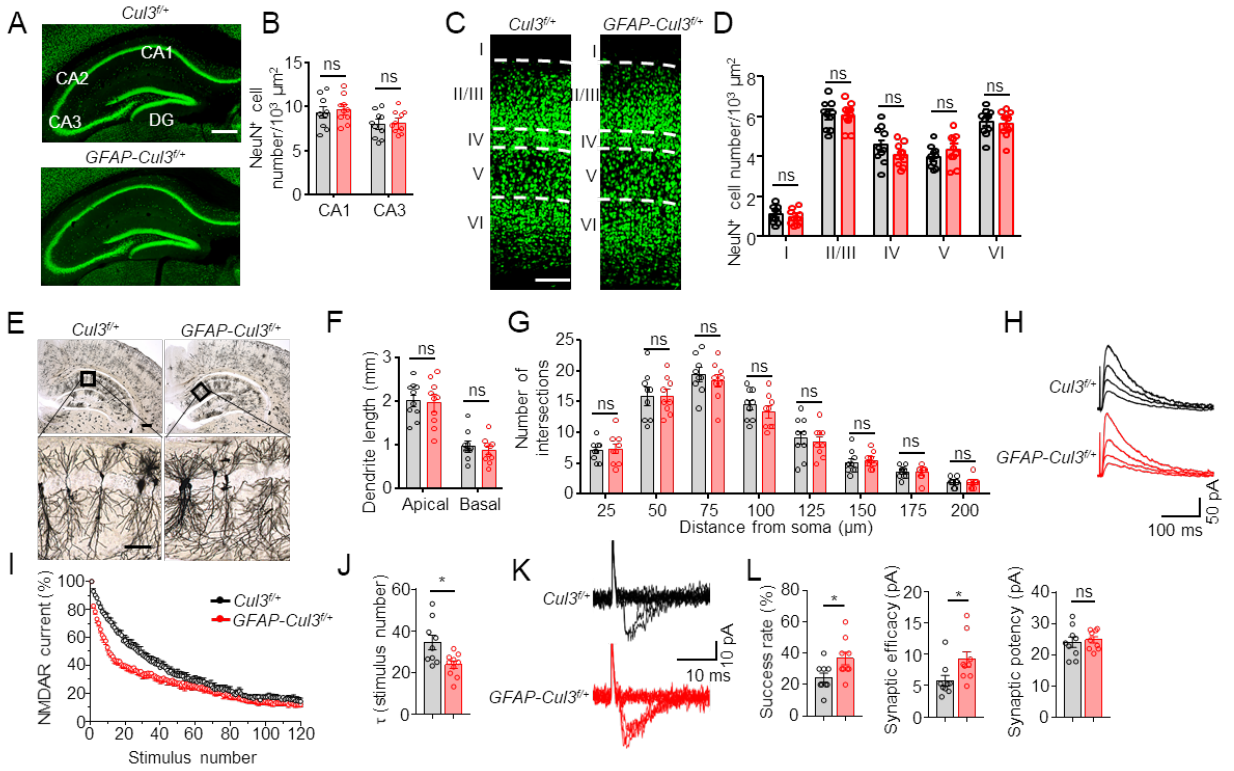

Figure S3. *GFAP-Cul3$^{f/+}$* mice displayed normal cortical development but enhanced glutamatergic release probability. Related to Figure 1. (A) Normal hippocampal morphology in *GFAP-Cul3$^{f/+}$* mice at P60. Sections were stained with antibody against NeuN. Scale bar, 500 μm (B) Quantification of NeuN-expressing cells in hippocampal CA1 and CA3 regions (n = 8 slices from 3 mice per genotype; *Cul3$^{f/+}$* vs *GFAP-Cul3$^{f/+}$* in CA1, p = 0.6164, U = 43; *Cul3$^{f/+}$* vs *GFAP-Cul3$^{f/+}$* in CA3, p = 0.7394, U = 45; Mann-Whitney test). (C) No apparent deficits in the somatosensory cortex of *GFAP-Cul3$^{f/+}$* mice at P60. Sections were stained with antibody against NeuN. Scale bar, 100 μm. (D) Quantification of NeuN-expressing neurons in the somatosensory cortex. n = 10 slices from 3 mice per genotype; *Cul3$^{f/+}$* vs *GFAP-Cul3$^{f/+}$* in I, p = 0.4927, U = 40.5; *Cul3$^{f/+}$* vs *GFAP-Cul3$^{f/+}$* in II/III, p = 0.8946, U = 48; *Cul3$^{f/+}$* vs *GFAP-Cul3$^{f/+}$* in IV, p =0.2176, U = 33; *Cul3$^{f/+}$* vs *GFAP-Cul3$^{f/+}$* in V, p = 0.4696, U = 40; for *Cul3$^{f/+}$* vs *GFAP-Cul3$^{f/+}$* in VI; p = 0.6990, U = 44.5; Mann-Whitney test. (E) Representative Golgi staining images of apical and basal dendrites in CA1 pyramidal neurons of control and *GFAP-Cul3$^{f/+}$* mice. Scale bar, 500 μm (upper panel) 100 μm (lower panel). (F) Quantitative analysis of dendrite length of apical and basal dendrites in CA1 pyramidal neurons (n = 10 neurons of 3 mice per genotype; *Cul3$^{f/+}$* vs *GFAP-Cul3$^{f/+}$* in Apical, p = 0.7394, U = 45; *Cul3$^{f/+}$* vs *GFAP-Cul3$^{f/+}$* in Basal, p = 0.6173, U = 43; Mann-Whitney test. (G) Quantitative analysis of dendritic complexity of CA1 pyramidal neurons by Sholl analysis. n = 9 neurons of three mice per genotype; p > 0.05 in all comparisons; Mann-Whitney test. (H) Representative traces of NMDAR currents in the presence of MK-801. (I) Normalized NMDAR currents plotted against stimulus number. (J) Decreased τ values in *GFAP-Cul3$^{f/+}$* mice. n = 9 neurons, 3 mice for *Cul3$^{f/+}$*; n = 10 neurons, 3 mice for *GFAP-Cul3$^{f/+}$*; *Cul3$^{f/+}$* (34.5 ± 4.6) vs *GFAP-Cul3$^{f/+}$* (23.7 ± 2.4), p = 0.0162; U = 16; Mann-Whitney test. (K) Representative 10 successive individual sweeps of EPSCs evoked by minimal stimulation. (L) Increased success rate, synaptic efficacy, and unaltered synaptic potency in *GFAP-Cul3$^{f/+}$* mice. n = 9 neurons from 3 mice per genotype; success rate, *Cul3$^{f/+}$* (24.4 ± 3.8) vs *GFAP-Cul3$^{f/+}$* (36.7 ± 3.4), p = 0.0369, U = 17; synaptic efficacy, *Cul3$^{f/+}$* (5.8 ± 1.2) vs *GFAP-Cul3$^{f/+}$* (9.2 ± 1.6), p = 0.0142, U = 13; synaptic potency, *Cul3$^{f/+}$* (24.1 ± 2.2) vs *GFAP-Cul3$^{f/+}$* (24.8 ± 1.4), p = 0.7304, U = 36; Mann-Whitney test. Data were shown as mean ± SEM. *p < 0.05; ns, no significant difference.

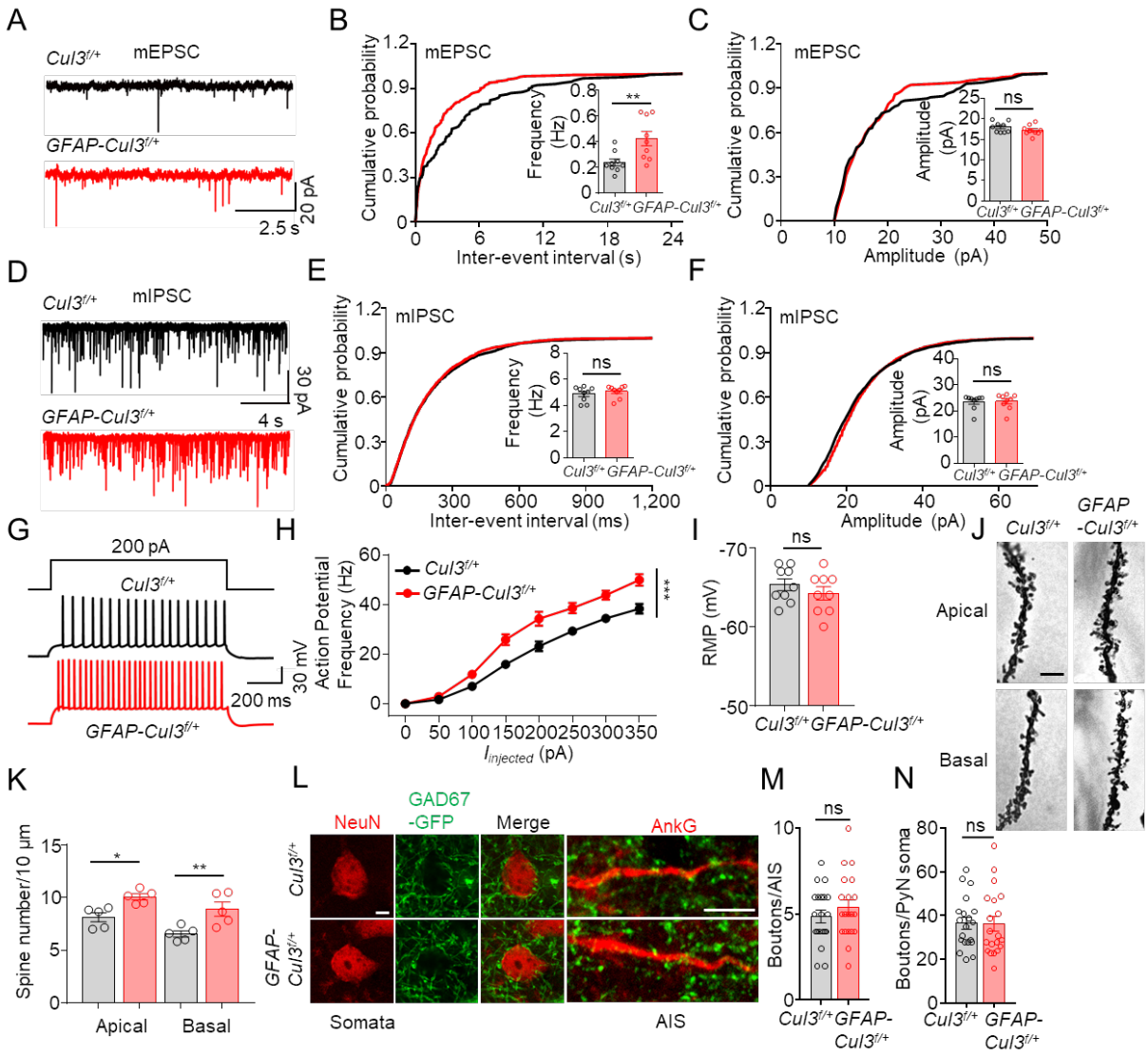

Figure S4. Disrupted CA1 E-I balance in immature (P14-17) *GFAP-Cul3$^{f/+}$* mice. Related to Figure 2. (A) Representative mEPSCs traces. (B) Increased mEPSC frequency. n = 9 neurons, 3 mice for both genotypes; *Cul3$^{f/+}$* (0.2 ± 0.02 Hz) vs *GFAP-Cul3$^{f/+}$* (0.4 ± 0.08 Hz), p = 0.0071; U = 11; Mann-Whitney test. (C) No difference in mEPSC amplitude. n = 9 neurons, 3 mice for both genotypes; p = 0.2313; U = 26.5; Mann-Whitney test. (D) Representative mIPSCs traces. (E) No difference in mIPSC frequency. n = 9 neurons, 3 mice for both genotypes; *Cul3$^{f/+}$* (17.9 ± 0.4 Hz) vs *GFAP-Cul3$^{f/+}$* (17.3 ± 0.4 Hz), p = 0.4484; U = 31.5; Mann-Whitney test. (F) No difference in mIPSC amplitude. n = 9 neurons, 3 mice for both genotypes; *Cul3$^{f/+}$* (23.5 ± 0.9 pA) vs *GFAP-Cul3$^{f/+}$* (23.7 ± 1.0 pA), p = 0.6665; U = 35; Mann-Whitney test. (G) Representative spikes traces evoked by depolarizing currents. (H) Firing rate plotted against increasing injected currents. n = 9 neurons, 3 mice for both genotypes; p < 0.0001; $F_{(1, 128)}$ = 70.54; Two-way ANOVA. (I) Comparable RMP of CA1 neurons. n = 9 neurons, 3 mice for both genotypes; p = 0.3653; U = 46; Mann-Whitney test. (J) Representative Golgi staining images of spines. Scale bar, 5 μm. (K) Increased spine density in apical and basal dendrites of CA1 *GFAP-Cul3$^{f/+}$* pyramidal neurons. n = 5 mice for both genotype; for spine density in apical dendrites, *Cul3$^{f/+}$* (8.1 ± 0.44) vs *GFAP-Cul3$^{f/+}$* (10.1 ± 0.29), p = 0.0079; U = 0; Mann-Whitney test; for spine density in basal dendrites, *Cul3$^{f/+}$* (6.6 ± 0.30) vs *GFAP-Cul3$^{f/+}$* (8.9 ± 0.67), p = 0.0159; U = 1; Mann-Whitney test. (L) Representative images of GAD67-GFP positive inhibitory synapses onto NeuN positive postsynaptic somata (square image in left; scale 5 μm) and representative images of GAD67-GFP positive inhibitory synapses onto AnkG positive axon initial segment (AIS) (rectangle image in right; scale 5 μm). (M) Quantification data of GABAergic boutons/AIS. n = 20 AIS of 3 mice per each genotype; p = 0.5070; U = 175.5; Mann-Whitney test. (N) Quantification data of GABAergic boutons/somata. n = 20 somata of 3 mice per each genotype; p = 0.6631; U = 183.5; Mann-Whitney test. Data were shown as mean ± SEM. *p < 0.05, **p < 0.01, ***p < 0.001; ns, no significant difference.

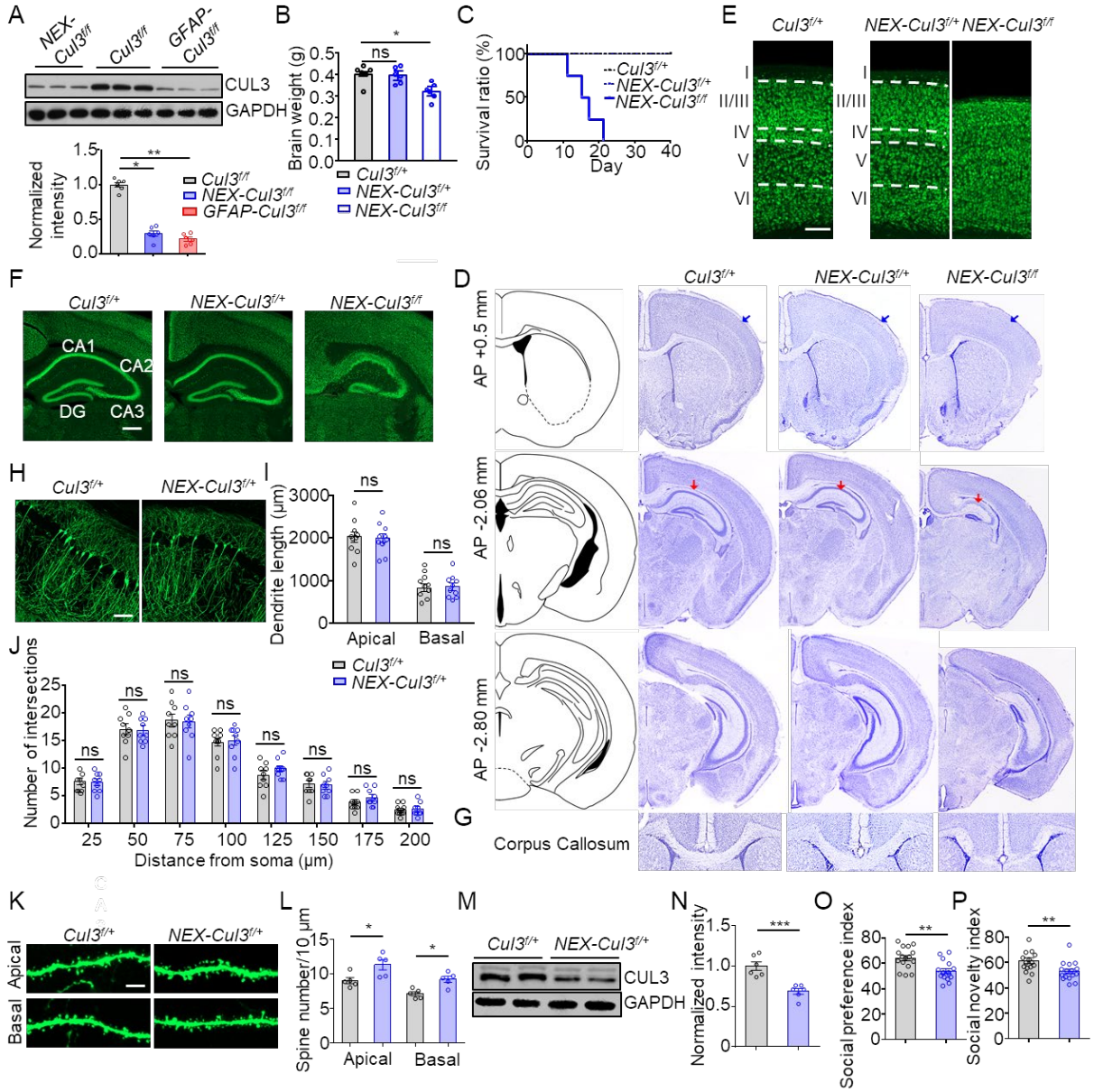

Figure S5. **Premature death and morphological deficits in the brain of *NEX-Cul3$^{f/f}$* mice and social deficits in *NEX-Cul3$^{f/+}$* mice. Related to Figure 3.** (A) Reduced CUL3 level in cortical homogenate of *GFAP-Cul3$^{f/f}$* and *NEX-Cul3$^{f/f}$* mice at the age of P14. n = 6 mice for each genotype; *Cul3$^{f/f}$* (1.0 ± 0.05) vs *NEX-Cul3$^{f/f}$* (0.3 ± 0.06), p = 0.0444; *Cul3$^{f/f}$* vs *GFAP-Cul3$^{f/f}$* (0.2 ± 0.05), p = 0.0019; Kruskal-Wallis ANOVA followed by Dunn's post hoc test. (B) Reduced brain weight of *NEX-Cul3$^{f/f}$* mice at the age of P14. n = 6 mice for each genotype; *Cul3$^{f/+}$* (0.4 ± 0.02) vs *NEX-Cul3$^{f/+}$* (0.4 ± 0.04), p > 0.9999; *Cul3$^{f/+}$* vs *NEX-Cul3$^{f/f}$* (0.3 ± 0.04), p = 0.0301; Kruskl-Wallis ANOVA followed by Dunn's post hoc test. (C) Reduced lifespan of *NEX-Cul3$^{f/f}$* mice. (D-G) Abnormal cortical structure, Scale bar, 1 mm (D), reduced cortical thickness, Scale bar, 100 μm (E), deformed hippocampus Scale bar, 500 μm. (F) and agenesis of the corpus callosum (G). (H) Representative image of hippocampal CA1 neurons visualized by Thy1-GFP. Scale bar, 100 μm. (I) Quantitative analysis of dendrite length of Apical and Basal dendrites in CA1 pyramidal neurons. n = 10 neurons of 3 mice per genotype; for *Cul3$^{f/+}$* vs *NEX-Cul3$^{f/+}$* in Apical, p = 0.7959, U = 46; for *Cul3$^{f/+}$* vs *NEX-Cul3$^{f/+}$* in Basal, p = 0.8534, U = 47; Mann-Whitney test. (J) Quantitative analysis of dendritic complexity of CA1 pyramidal neurons by Sholl analysis. n = 9 neurons of three mice per genotype; p > 0.05 in all comparisons; Mann-Whitney test. (K) Representative images of apical and basal spines of hippocampus CA1 pyramidal neurons. Spines were visualized by Thy1-GFP and those on the secondary/tertiary branches were counted. Scale bar, 5 μm. (L) Increased spine density in apical and basal dendrites of CA1 *NEX-Cul3$^{f/+}$* pyramidal neurons. n = 5 mice per genotype; for spine density in apical dendrites, *Cul3$^{f/+}$* (9 ± 0.5) vs *NEX-Cul3$^{f/+}$* (11.3 ± 0.7), p = 0.0317; U = 2; spine density in basal

dendrites, *Cul3*$^{f/+}$ (7.1 ± 0.3) vs *NEX-Cul3*$^{f/+}$ (9 ± 0.5), p < 0.0159; U = 1; Mann-Whitney test. (M) Representative blots on CUL3 expression. (N) Reduced CUL3 expressions in P60 *NEX-Cul3*$^{f/+}$ mice cortical tissues. n = 5 mice per each group; GAPDH was used as loading controls; *Cul3*$^{f/+}$ (1.0 ± 0.05) vs *NEX-Cul3*$^{f/+}$ (0.7 ± 0.04), p = 0.0006; Student's t test. (O) Social preference index in *NEX-Cul3*$^{f/+}$ mice. n = 16 mice per genotype; *Cul3*$^{f/+}$ (64.1 ± 2.1) vs *NEX-Cul3*$^{f/+}$ (53.8 ± 1.9), p = 0.003; U = 52; Mann-Whitney test. (P) Social novelty index in *NEX-Cul3*$^{f/+}$ mice. n = 16 mice per genotype; *Cul3*$^{f/+}$ (61.3 ± 2.3) vs *NEX-Cul3*$^{f/+}$ (53.0 ± 1.9), p = 0.0045; U = 54; Mann-Whitney test. Data were shown as mean ± SEM. *p < 0.05, **p < 0.01, ***p < 0.001; ns, no significant difference.

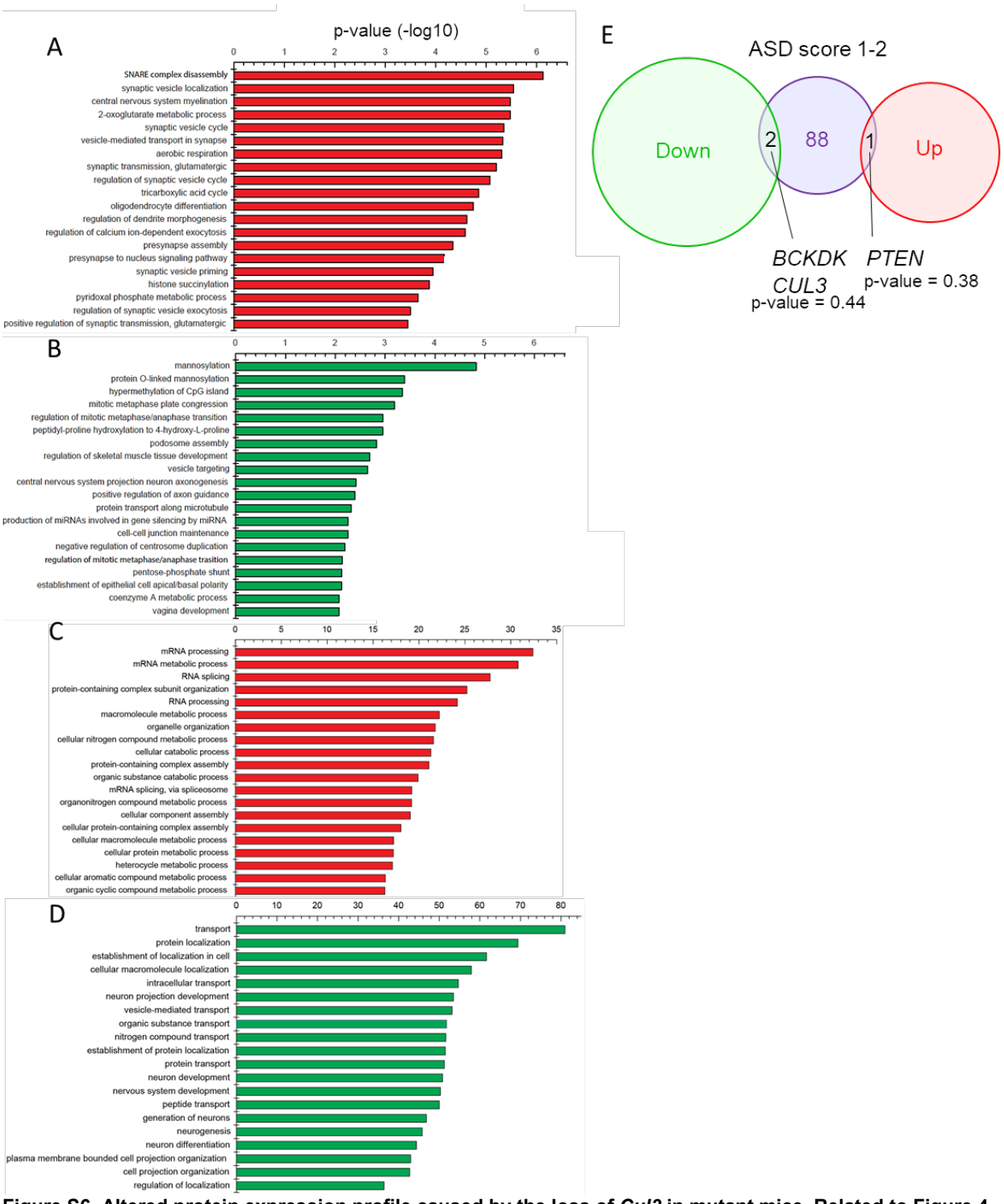

Figure S6. **Altered protein expression profile caused by the loss of *Cul3* in mutant mice. Related to Figure 4.** (A) GO- 'Biological process' analysis on upregulated proteins identified in proteomics analysis, by comparing *GFAP-Cul3$^{f/+}$* mice vs. *Cul3$^{f/+}$* mice. (B) GO- 'Biological process' analysis on downregulated proteins identified in proteomics analysis, by comparing *GFAP-Cul3$^{f/+}$* mice vs. *Cul3$^{f/+}$* mice. (C) GO- 'Biological process' analysis on upregulated proteins identified in proteomics analysis, by comparing *GFAP-Cul3$^{f/f}$* mice vs. *Cul3$^{f/+}$* mice. (D) GO- 'Biological process' analysis on downregulated proteins identified in proteomics analysis, by comparing *GFAP-Cul3$^{f/f}$* mice vs. *Cul3$^{f/+}$* mice. (E) DE proteins that overlapped with high confident SFARI genes (score 1 and 2 only). Data were analyzed by Fisher's exact test.

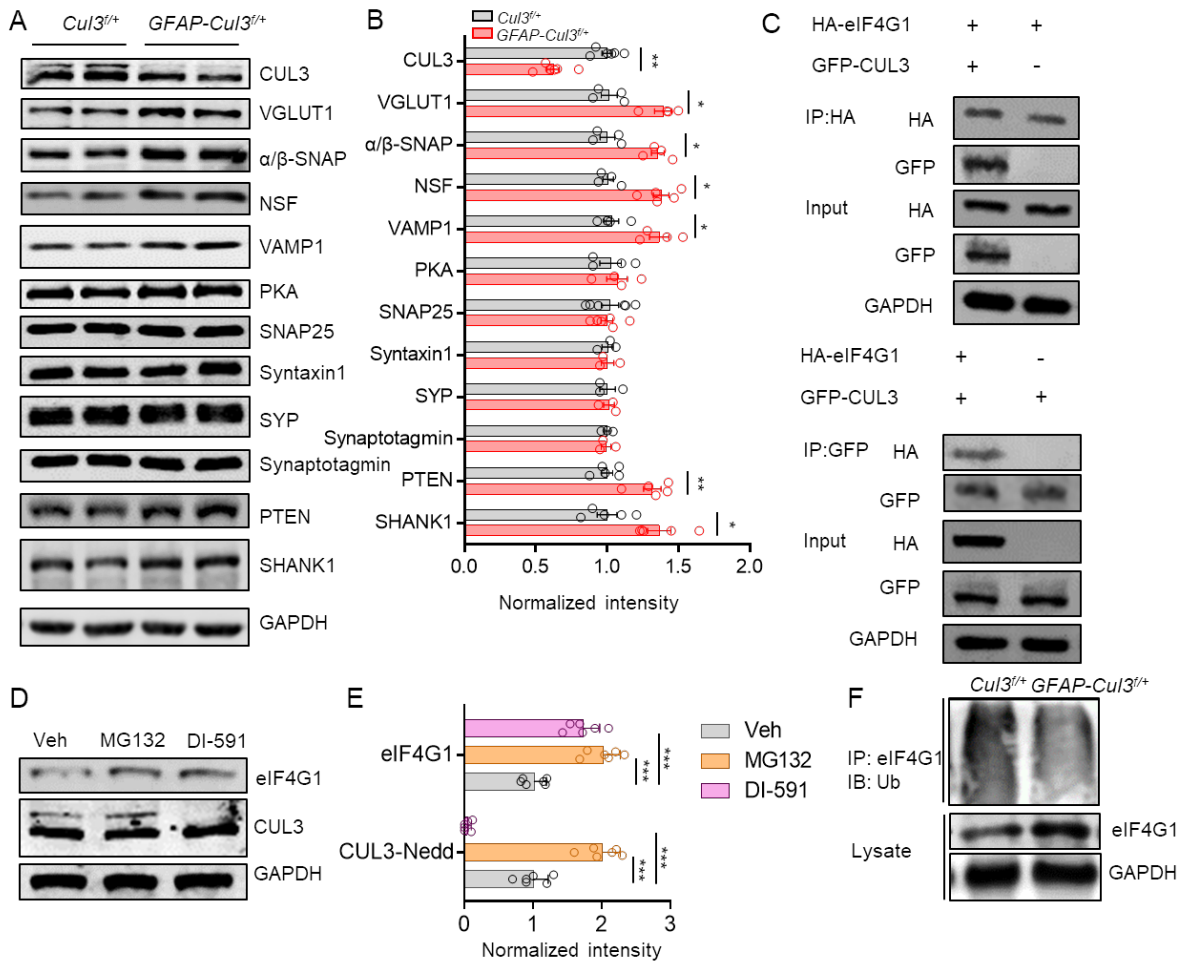

Figure S7. Enhanced protein translation and reduced eIF4G1 ubiquitination in *GFAP-Cul3$^{f/+}$* neurons. Related to Figure 4. (A, B) Western blot analysis of interested proteins in the cortex. A, Representative blots. B, Quantitative data. n = 3-6 mice per genotypes; GAPDH was used for loading controls; *Cul3$^{f/+}$* (1.0 ± 0.05) vs *GFAP-Cul3$^{f/+}$* (1.35 ± 0.05), p = 0.0286, U_{VAMP1} = 0; *Cul3$^{f/+}$* (1.0 ± 0.06) vs *GFAP-Cul3$^{f/+}$* (1.38 ± 0.03), p = 0.0159, U_{NSF} = 0; *Cul3$^{f/+}$* (1.0 ± 0.05) vs *GFAP-Cul3$^{f/+}$* (1.32 ± 0.06), p = 0.0286, $U_{α/β\text{-}SNAP}$ = 0; *Cul3$^{f/+}$* (1.0 ± 0.06) vs *GFAP-Cul3$^{f/+}$* (1.41 ± 0.06), p = 0.0286, U_{VGLUT1} = 0; *Cul3$^{f/+}$* (1.0 ± 0.04) vs *GFAP-Cul3$^{f/+}$* (0.62 ± 0.04), p = 0.0022, U_{CUL3} = 0; *Cul3$^{f/+}$* (1.0 ± 0.07) vs *GFAP-Cul3$^{f/+}$* (1.35 ± 0.09), p = 0.019, U_{SHANK1} = 0; *Cul3$^{f/+}$* (1.0 ± 0.04) vs *GFAP-Cul3$^{f/+}$* (1.29 ± 0.06), p= 0.0079, U_{PTEN} = 0; Mann-Whitney test. (C) Co-immunoprecipitation of CUL3 and eIF4G1. HEK293T cells were co-transfected with HA-eIF4G1 and GFP-CUL3. HA or GFP antibodies were used for immunoprecipitation. (D, E) Increased eIF4G1 in neurons treated by MG132 or DI-591. MG132 (10 μM) or DI-591 (10 μM) was added into culture medium at DIV14 for 48 h. D, Representative blot; E, Quantitative data. n = 6 samples per each group; GAPDH was used for loading controls; for CUL3-Nedd, Veh (1.0 ± 0.10) vs MG132 (2.0 ± 0.12), p < 0.001; Veh vs DI-591 (0.05 ± 0.02), p < 0.001; for eIF4G1, Veh (1.0 ± 0.08) vs MG132 (2.0 ± 0.11), p < 0.001; Veh vs DI-591 (1.7 ± 0.11), p < 0.001; One-way ANOVA followed by Tukey's post hoc test. (F) Reduced eIF4G1 ubiquitination in *GFAP-Cul3$^{f/+}$* cortex. eIF4G1 antibody was used for immunoprecipitation and Ub antibody was used for immunoblotting. Data were shown as mean ± SEM. *p < 0.05, **p < 0.01; ns, no significant difference.

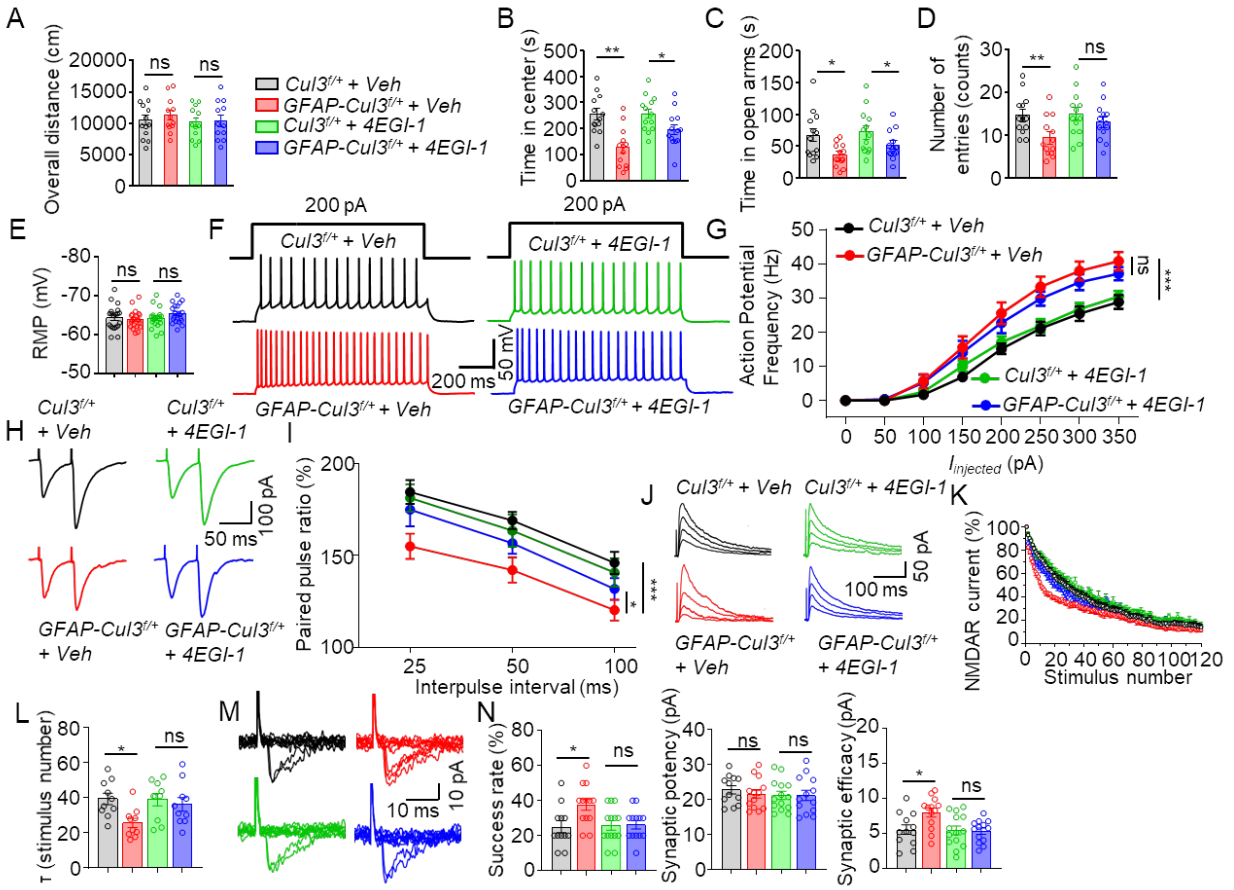

Figure S8. **4EGI-1 failed to rescue neuronal excitability and anxiety phenotypes in CUL3 deficiency mice but attenuated glutamate release probability in CUL3 deficient neurons. Related to Figure 5.** (A) No effect of 4EGI-1 was found on total distance traveled in open field test. n = 13 mice for each group; p > 0.9999 for all comparisons; Kruskal-Wallis ANOVA followed by Dunn's post hoc test. (B) No effect of 4EGI-1 was found on time spent in center by *GFAP-Cul3*$^{f/+}$ mice in open field test. n = 13 mice for each group; for Veh-treated *Cul3*$^{f/+}$ (251 ± 25.2 s) vs Veh-treated *GFAP-Cul3*$^{f/+}$ (133 ± 21.6 s), p = 0.0020; for 4EGI-1-treated *Cul3*$^{f/+}$ (252 ± 18.3 s) vs 4EGI-1-treated *GFAP-Cul3*$^{f/+}$ (204 ± 19.5 s), p = 0.0418; Kruskal-Wallis ANOVA followed by Dunn's post hoc test. (C) No effect of 4EGI-1 was found on time in open arms of *GFAP-Cul3*$^{f/+}$ mice in EPM test. n = 13 mice for each group; for Veh-treated *Cul3*$^{f/+}$ (63.4 ± 8.2 s) vs Veh-treated *GFAP-Cul3*$^{f/+}$ (37.3 ± 6.4 s), p = 0.0350; for 4EGI-1-treated *Cul3*$^{f/+}$ (72.7 ± 10.1 s) vs 4EGI-1-treated *GFAP-Cul3*$^{f/+}$ (51.3 ± 7.1 s), p = 0.0430; Kruskal-Wallis ANOVA followed by Dunn's post hoc test. (D) 4EGI-1 abolished difference in number of entries into open arms between control and *GFAP-Cul3*$^{f/+}$ mice in EPM test. n = 13 mice for each group; for Veh-treated *Cul3*$^{f/+}$ (14.4 ± 1.6) vs Veh-treated *GFAP-Cul3*$^{f/+}$ (9.7 ± 1.7), p = 0.0062; for 4EGI-1-treated *Cul3*$^{f/+}$ (15.3 ± 1.4) vs 4EGI-1-treated *GFAP-Cul3*$^{f/+}$ (13.8 ± 1.3), p > 0.9999; Kruskal-Wallis ANOVA followed by Dunn's post hoc test. (E) RMP of recorded CA1 pyramidal neurons from control and *GFAP-Cul3*$^{f/+}$ mice. n = 18-21 neurons from 4 mice per each group infused with Veh or 4EGI-1 (50 μM, 0.5 μl) bilaterally. (F) Representative traces of spikes in CA1 pyramidal neurons evoked by injecting depolarizing currents of 200 pA. (G) Firing rate plotted against increasing injected currents. n = 9 neurons, 3 mice for both genotypes; Veh-treated *Cul3*$^{f/+}$ vs Veh-treated *GFAP-Cul3*$^{f/+}$, p < 0.001; Veh-treated *GFAP-Cul3*$^{f/+}$ vs 4EGI-1-treated *GFAP-Cul3*$^{f/+}$, p < 0.3585; $F_{(3, 256)}$ = 26.46; Two-way ANOVA followed by Bonferroni's post hoc test. (H) Representative traces of pair-pulse stimulations. (I) PPRs of *GFAP-Cul3*$^{f/+}$ neurons were increased by 4EGI-1. PPRs were plotted against inter-stimulus intervals. n = 13-14 neurons, 3 mice for all groups; Veh-treated *Cul3*$^{f/+}$ vs Veh-treated *GFAP-Cul3*$^{f/+}$, p < 0.001; Veh-treated *GFAP-Cul3*$^{f/+}$ vs 4EGI-1-treated *GFAP-Cul3*$^{f/+}$, p = 0.0459; 4EGI-1-treated *Cul3*$^{f/+}$ vs 4EGI-1-treated *GFAP-Cul3*$^{f/+}$, p > 0.9999; $F_{(3,153)}$ = 9.236, Two-way ANOVA followed by Bonferroni's post hoc test. (J) Representative traces of NMDAR currents in the presence of MK-801. (K) Normalized NMDAR currents plotted against stimulus number. (L) 4EGI-1 restored low τ values in *GFAP-Cul3*$^{f/+}$ mice. n = 10 neurons, 3 mice per each groups; Veh-treated *Cul3*$^{f/+}$ (39.3 ± 3.2) vs Veh-treated *GFAP-Cul3*$^{f/+}$ (25.6 ± 2.7), p = 0.031; 4EGI-1-treated *Cul3*$^{f/+}$ (38.9 ± 3.5) vs 4EGI-1-treated *GFAP-Cul3*$^{f/+}$ (36.2 ± 3.9), p = 0.9421; Kruskal-Wallis ANOVA followed by Dunn's post hoc test. (M) Representative 10 successive individual sweeps of EPSCs evoked by minimal stimulation. (N) 4EGI-1 attenuated high success rate, synaptic efficacy, and unaltered synaptic potency in *GFAP-Cul3*$^{f/+}$ mice. n = 12 neurons, 3 mice for Veh-treated

Cul3$^{f/+}$, n = 13 neurons, 3 mice for and Veh-treated *GFAP-Cul3*$^{f/+}$ and 4EGI-1-treated *GFAP-Cul3*$^{f/}$, n = 14 neurons, 3 mice for 4EGI-1-treated *Cul3*$^{f/+}$; success rate, Veh-treated *Cul3*$^{f/+}$ (23.2 ± 3.5) vs Veh-treated *GFAP-Cul3*$^{f/+}$ (38.3 ± 2.1), p = 0.0213; 4EGI-1-treated *Cul3*$^{f/+}$ (24.7 ± 1.7) vs 4EGI-1-treated *GFAP-Cul3*$^{f/+}$ (25.1 ± 1.6), p = 0.741; synaptic efficacy, Veh-treated *Cul3*$^{f/+}$ vs Veh-treated *GFAP-Cul3*$^{f/+}$, p = 0.713; 4EGI-1-treated *Cul3*$^{f/+}$ vs 4EGI-1-treated *GFAP-Cul3*$^{f/+}$, p = 0.508; synaptic potency, Veh-treated *Cul3*$^{f/+}$ (5.1 ± 0.8) vs Veh-treated *GFAP-Cul3*$^{f/+}$ (7.6 ± 0.6), p = 0.011; 4EGI-1-treated *Cul3*$^{f/+}$ (5.1 ± 0.7) vs 4EGI-1-treated *GFAP-Cul3*$^{f/+}$ (5.0 ± 0.5), p = 0.893; Kruskal-Wallis ANOVA followed by Dunn's post hoc test. Data were shown as mean ± SEM. *p < 0.05, **p < 0.01, ***p < 0.001; ns, no significant difference.

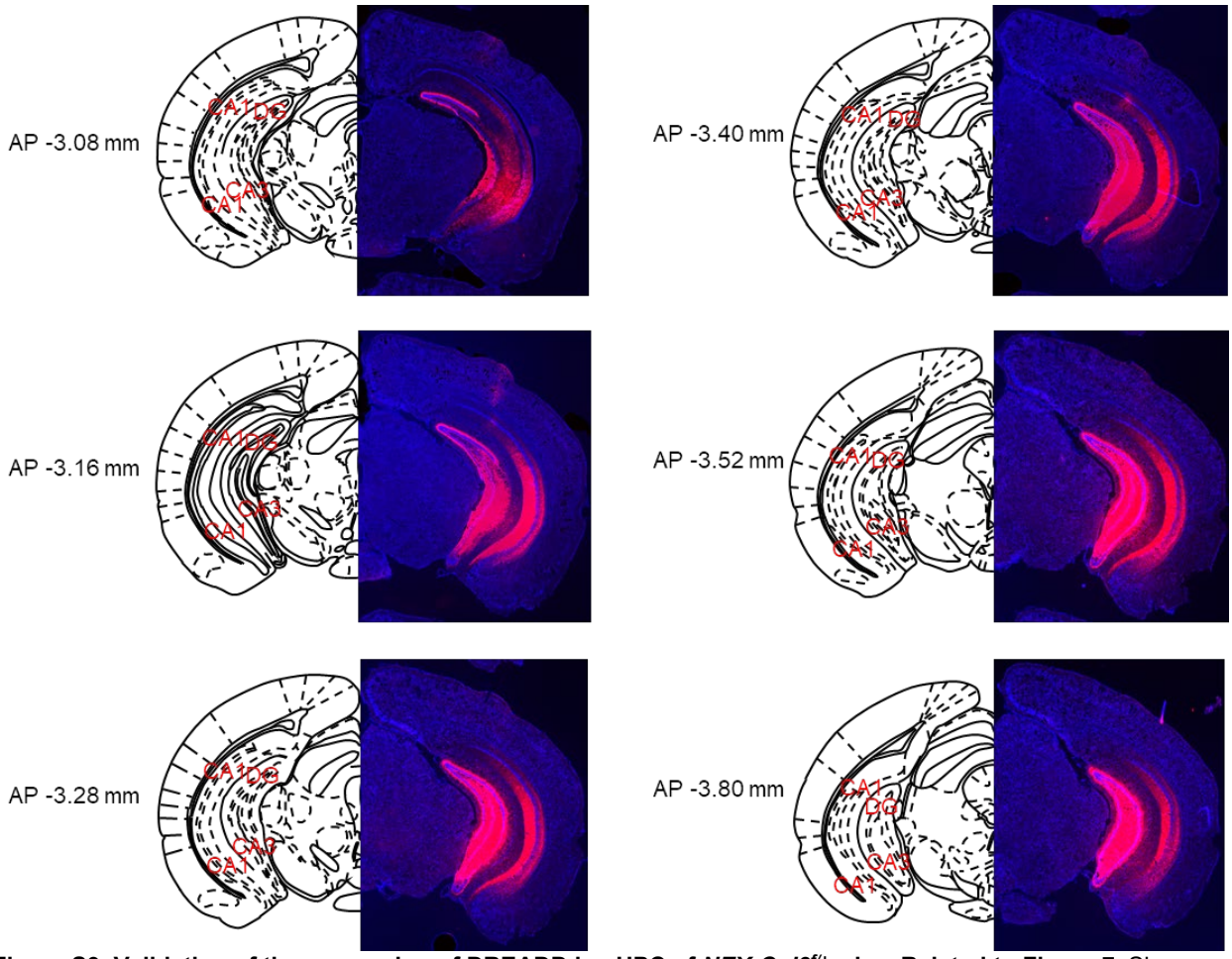

Figure S9. **Validation of the expression of DREADD in vHPC of *NEX-Cul3*$^{f/+}$ mice. Related to Figure 7**. Shown were serial sections of vHPC at different coordinates from injected mice. Brain atlas was shown on the left.

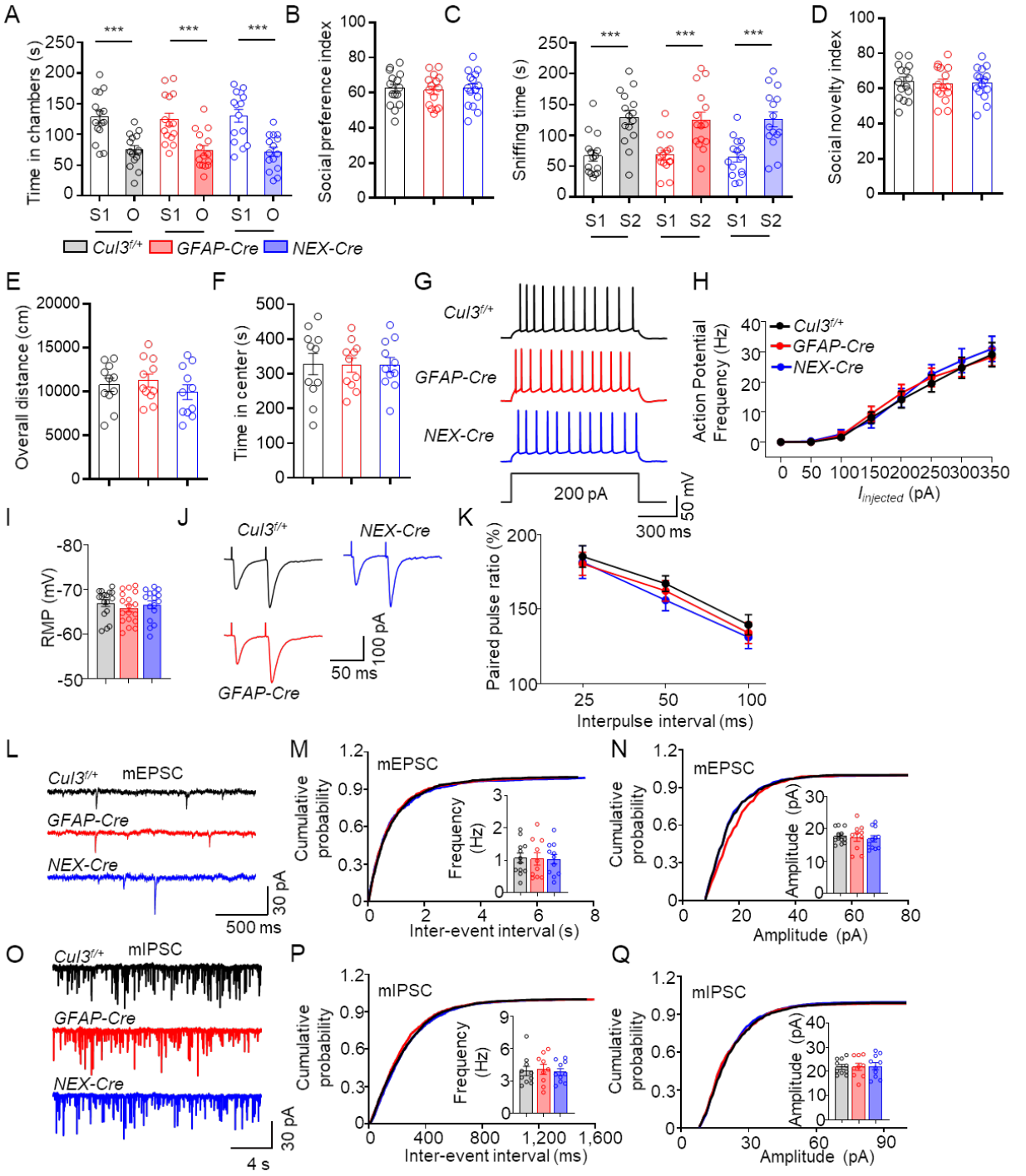

Figure S10. **Validation of behavioral and neuronal properties of *GFAP-Cre* and *NEX-Cre* mice. Related STAR Method.** (A) No difference in social preference between *Cul3*$^{f/+}$, *GFAP-Cre* and *NEX-Cre* mice. n = 15 mice for each group; *Cul3*$^{f/+}$ S1 (128 ± 10.1 s) vs *Cul3*$^{f/+}$ O (74.7 ± 7.1 s), p < 0.001; *GFAP-Cre* S1 (125 ± 73.9 s) vs *GFAP-Cre* O (73.9 ± 7.9 s), p < 0.001; *NEX-Cre* S1 (131 ± 10.4 s) vs *NEX-Cre* O (71.6 ± 7.5 s), p < 0.001; Two-way ANOVA followed by Bonferroni's post hoc test. (B) No difference in social preference index preference between *Cul3*$^{f/+}$, *GFAP-Cre* and *NEX-Cre* mice. n = 15 mice per each group; p = 0.761; Kruskal-Wallis ANOVA followed by Dunn's post hoc test. (C) No difference in social memory between *Cul3*$^{f/+}$, *GFAP-Cre* and *NEX-Cre* mice. n = 15 mice for each group; *Cul3*$^{f/+}$ S1 (66.9 ± 8.7 s) vs *Cul3*$^{f/+}$ S2 (129 ± 11.3 s), p < 0.001; *GFAP-Cre* S1 (68.3 ± 124.9 s) vs *GFAP-Cre* S2 (125 ± 12.5 s), p < 0.001; *NEX-Cre* S1 (64.9 ± 8.0 s) vs *NEX-Cre* S2 (126 ± 12.3 s), p < 0.001; Two-way ANOVA followed by Bonferroni's post hoc test. (D) No difference in social preference index preference between

Cul3$^{f/+}$, *GFAP-Cre* and *NEX-Cre* mice. n = 15 mice per each group; p = 0.808; Kruskal-Wallis ANOVA followed by Dunn's post hoc test. (E) No difference in total distance traveled. n = 11 mice for each group; p = 0.796; Kruskal-Wallis ANOVA followed by Dunn's post hoc test. (F) Similar time spent in the center. n = 11 mice for each group; p = 0.728; Kruskal-Wallis ANOVA followed by Dunn's post hoc test. (G) Representative traces of spikes evoked by injecting depolarizing currents. (H) Firing rates plotted against increasing injected currents. n = 10 neurons, 3 mice for *Cul3*$^{f/+}$ and *GFAP-Cre* mice; n = 9 neurons, 3 mice for *NEX-Cre* mice; p = 0.713; Two-way ANOVA followed by Bonferroni's post hoc test. (I) Comparable resting membrane potentials of CA1 pyramidal neurons. n = 16-18, 3 mice for all genotypes; p = 0.699; One-way ANOVA followed by Tukey's post hoc test. (J) Representative traces of pair-pulse stimulation. (K) PPRs plotted against inter-stimulus intervals. n = 9-10 neurons, 3 mice per each group; p = 0.881; Two-way ANOVA followed by Bonferroni's post hoc test. (L) Representative mEPSC traces in CA1 pyramidal neurons. (M) No difference in mEPSC frequency. n = 12 neurons, 3 mice for *Cul3*$^{f/+}$ mice; n = 10 neurons, 3 mice for *GFAP-Cre* mice; n = 11 neurons, 3 mice for *NEX-Cre* mice; p > 0.999; One-way ANOVA followed by Tukey's post hoc test. (N) No difference in mEPSC amplitude. n = 12 neurons, 3 mice for *Cul3*$^{f/+}$ mice; n = 10 neurons, 3 mice for *GFAP-Cre* mice; n = 11 neurons, 3 mice for *NEX-Cre* mice; p = 0.911; One-way ANOVA followed by Tukey's post hoc test. (O) Representative mIPSC traces in CA1 pyramidal neurons. (P) No difference in mIPSC frequency. n = 10 neurons, 3 mice for *Cul3*$^{f/+}$ and *NEX-Cre* mice; n = 9 neurons, 3 mice for *GFAP-Cre* mice; p = 0.903; One-way ANOVA followed by Tukey's post hoc test. (Q) No difference in mIPSC amplitude. n = 10 neurons, 3 mice for *Cul3*$^{f/+}$ and *NEX-Cre* mice; n = 9 neurons, 3 mice for *GFAP-Cre* mice; p > 0.999; One-way ANOVA followed by Tukey's post hoc test. Data were shown as mean ± SEM. ns, no significant difference.